

Synthesis and Thermo-Electric Properties of Nb₂PdS₅ Superconductor In Bulk.

Anil K. Yadav

*Department of Physics, Ch. Charan Singh University,
Meerut, India-560012*

*Department of Physics, Indian Institute of Technology Bombay,
Mumbai, India- 400076*

anilphy@ccsuniversity.ac.in

Veg Singh Bhatt

*Department of Physics, Ch. Charan Singh University,
Meerut, India-560012*

Sandeep Yadav

*Department of Physics, Baba Mastnath University Asthal Bohar,
Rohtak-124021*

C. V. Tomy

*Department of Physics, Indian Institute of Technology Bombay,
Mumbai, India- 400076*

Corresponding Author: Anil K. Yadav

Copyright © 2023 Anil K. Yadav, et al. This is an open access article distributed under the Creative Commons Attribution License, which permits unrestricted use, distribution, and reproduction in any medium, provided the original work is properly cited.

Abstract

We report synthesis and thermal transport properties of ternary chalcogenide, Nb₂PdS₅ superconducting compound at low and room temperatures via thermo-electric measurements. Polycrystalline sample was synthesized via conventional solid-state reaction method. Seebeck coefficient (S) abruptly changes near superconducting transition temperature ($T_c \sim 6.5$ K). The positive value of S indicates the presence of holes like charge carriers in majority in normal state. The figure of merit, an essential qualitative parameter of thermo-electric materials, increases from low temperature towards the room temperature.

Keywords: Polycrystalline, Thermoelectric material, Seebeck coefficient, Superconductivity

1. INTRODUCTION

Nb-based non- superconducting ternary chalcogenide Nb₂Pd_{0.81}Se₅ compound exhibits superconductivity at transition temperature, $T_c \sim 6.5$ K by substituting S in place of Se [1], and crystallized in monoclinic iso-structure like Nb₂PdS₅ of C2/m space group [1–3]. This superconducting compound has been got attention due to showing extremely large upper critical field (H_{c2}) among reported Nb-based superconductors [1–6]. The highest upper critical field (H_{c2}), at which superconductivity

sustain, has been reported ~ 240 kOe in polycrystalline Nb_2PdS_5 superconductor [1, 3], higher than Pauli Paramagnetic limit ($H_{c2} \sim 1.84T_c$) [7]. Andreev reflection spectroscopic measurements revealed its two band nature of superconductor like MgB_2 [7, 8] and nodeless superconducting gap in quasi 1-D, preserved time reversal symmetry [9]. These superconductors Cooper pair have *s*-wave superconducting order parameter [10]. Fermi surface of compound consists multiple sheets of both electron and holes thus theoretically also reported through DFT band structure calculations as multi-band superconductor [1, 11]. It is further corroborated in Andreev spectroscopy and transport measurements [12, 13]. The type of Fermi surface is resembled to the Fe-based superconductors whereas contradicts to the cuprate superconductors [3, 4]. Various research groups have tried to enhance the transition temperature via doping or substitution of chemical elements such as Ir, Pt, Ru and Ni at Pd site, these have slightly modified the T_c , and however Ag, and Ni completely suppressed superconductivity [1, 14–18]. Vinay et al., have reported the enhancement of the upper critical field by doping of Te at S site [19]. Jennifer et al., have studied doping concentration of Pd thoroughly in $\text{Nb}_2\text{Pd}_x\text{Se}$ structure and reported that Pd is intercalated into the structure, also confirmed from DFT [20]. During single crystal formation, this compound in form of fiber, one group has tried to make flexible fiber by coating it on paper [21]

Keeping in mind above studies, thermal-transport nature of the compound have been left to explore by which one may predict type of majority of charge carriers present in Fermi-surface before entering in superconducting phase. We have performed electrical and thermal transport measurements within superconducting as well as in normal states. This study also explore figure of merit of this compound which concern with conversion of heat energy into electrical energy.

2. EXPERIMENTAL TECHNIQUES

Polycrystalline sample of Nb_2PdS_5 were synthesized via conventional solid state reaction method as reported in references [3, 6]. Initial ingredients of high purity Nb(4N), Pd(4N) and S(5N) were taken from Alfa Aesar in desired stoichiometry and homogenized in agate/mortar. Fine homogenized grinded powder was filled in double wall quartz tube followed by evacuation up to 10^{-5} torr. Sealed evacuated quartz tube was loaded in a high temperature furnace and heated with the rate of 10°C/h for solid state reaction at temperature 800°C for 24 hours. Powder X-ray diffraction (XRD) was performed in Philips X'Pert Pro diffractometer with Cu-K radiation for phase purity analysis. Thermal transport and heat capacity measurements were performed in PPMS (Quantum Design Inc., USA).

3. RESULTS AND DISCUSSIONS

3.1 Structure Analysis

FIGURE 1 shows the powder XRD pattern of Nb_2PdS_5 sample along with Rietveld refinements results. The Rietveld refinement was performed in X'Pert plus software using monoclinic crystal lattice of C2/m space group as reference (ICSD: 53315) with atomic positions: Nb1: $4i(0.582, 0, 0.183)$, Nb2: $4i(0.156, 0, 0.378)$, Pd1: $2a(0, 0, 0)$, Pd2: $2c(0, 0, 0.5)$ and S5 (*x,y,z*) and temperature parameter $B = 0.5$. All intensity peaks are well matched with reference pattern. The lattice

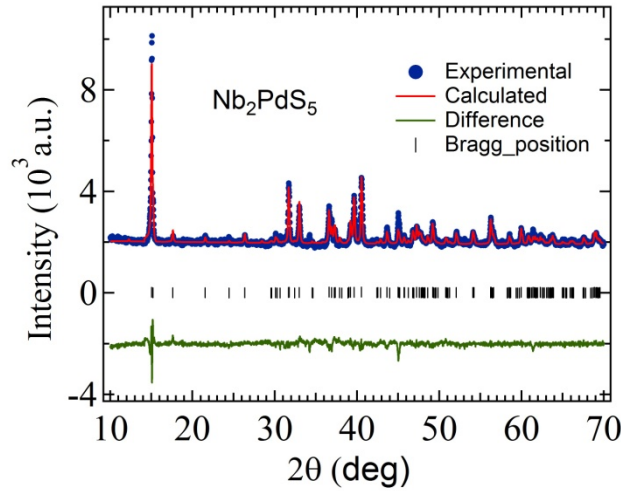


Figure 1: X-ray diffraction patterns of Nb_2PdS_5 polycrystalline sample. Peaks are well matched with monoclinic crystal structure of $C2/m$ space group.

parameters are coming out from refinement and found to be, $a = 12.14(7) \text{ \AA}$, $b = 3.28(1) \text{ \AA}$ and $c = 15.08(4) \text{ \AA}$ with $\chi^2 = 2.640$, comparable to previous published results [1–3].

3.2 Thermal Transport Properties

FIGURE 2(a) depicts the thermal conductivity (κ) measurements as a function of temperature in the range 2 – 300 K of Nb_2PdS_5 compound. In low temperature regime, $\kappa(T)$ gradually increases with increasing temperature and attains maximum κ near 120 K. This is the typical behavior in thermal conductivity found for the metal and alloys, further limits arises due to the scattering of conducting electrons from grain boundaries [22]. The nature of $\kappa(T)$ curve is found reminiscent with the MgB_2 superconductor [23]. In metal, electrons and phonons, both are responsible for the transport of thermal energy. Contribution from electron only can be explained by Wiedemann-Franz Law *i.e.*, $K_e = L_0 T / \rho$, where $L_0 (= 2.45 \times 10^{-8} \text{ W/M-K})$ is the Lorentz constant. Inset of FIGURE 2(a) shows the thermal conductivity at zero and 90 kOe magnetic fields within superconducting state. The higher field the $\kappa(T)$ curve deviates from zero field curve as magnetic field break the Cooper pairs and generate free electrons [23]. FIGURE 2(b) depicts the Seebeck coefficient (S) measurements as function of temperature in the range 2 - 300 K at zero magnetic fields. The variation of S with T is comparable with metallic compound. In superconducting state, initial $S(T)$ increases sharply with temperature and reach maximum $S \sim 17.8 \mu\text{V/K}$ at 43 K further, S decrease gradually up to 100 K and rises again to attain maximum $S \sim 20.0 \mu\text{V/K}$ at 300 K.

This thermoelectric trend can be explained using the concept of diffusion (S_d) and phonon-drag (S_{ph}) components [22, 24]. In low temperature regime, say below Debye temperature, the S_{ph} varies as third power of temperature in addition with diffusion component and above this temperature, S_d varies inversely with temperature [24]. The sign S can be negative or positive that refers

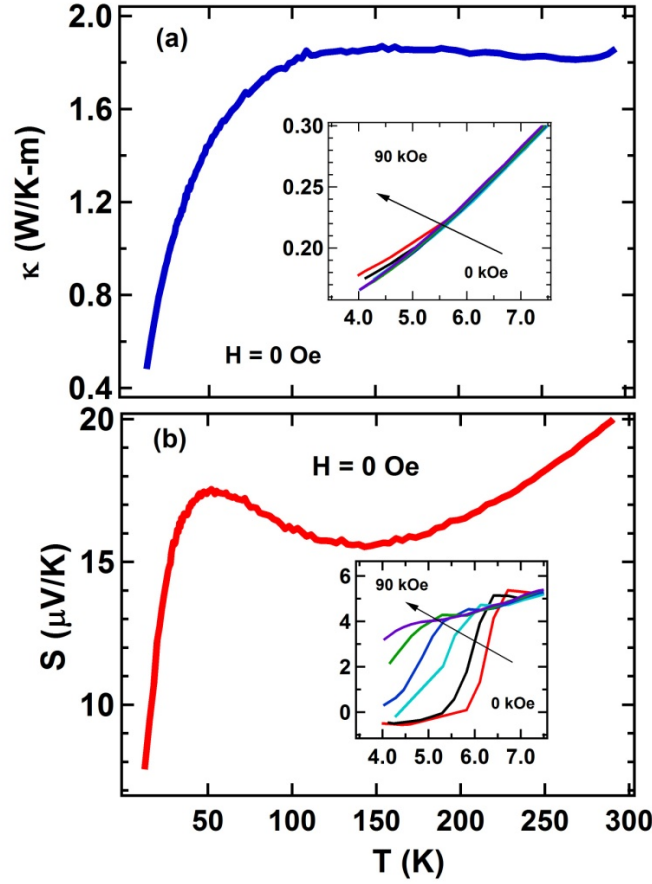


Figure 2: (a) Thermal conductivity vs temperature plot at zero magnetic field (b) Seebeck coefficient (S) vs temperature plot at zero magnetic field.

type of charge carriers in normal state [25], here, positive sign of S suggests that holes are dominant charge carriers available for thermal conduction in normal state [1, 11, 26].

Thermo power relation with Fermi temperature is used to probe the correlation strength of system. Following the Fermi-liquid theory, Behania *et al.*, [26] have reported that diffusive Seebeck component should be linear with temperature in low temperature limit and magnitude at zero temperature provide strength of electronic correlation,

$$S/T = (\pm\pi^2 k_B)/2eT_F$$

where k_B is Boltzmann's constant, e electron charge and T_F is Fermi temperature, it is similar to electronic specific heat response with temperature i.e. $C_{el}/T = \gamma$, at zero temperature limit, where γ tells about electronic correlation strength. To get the value of S/T at zero-temperature limit, the data of S/T at higher temperature fitted linearly and further extrapolated lower to zero temperature. The quantitative value of S/T at zero-temperature limit was found to be $0.79 \mu\text{V/K}^2$ from fitting parameters and corresponding estimated Fermi temperature (T_F) is 538 K using above equation.

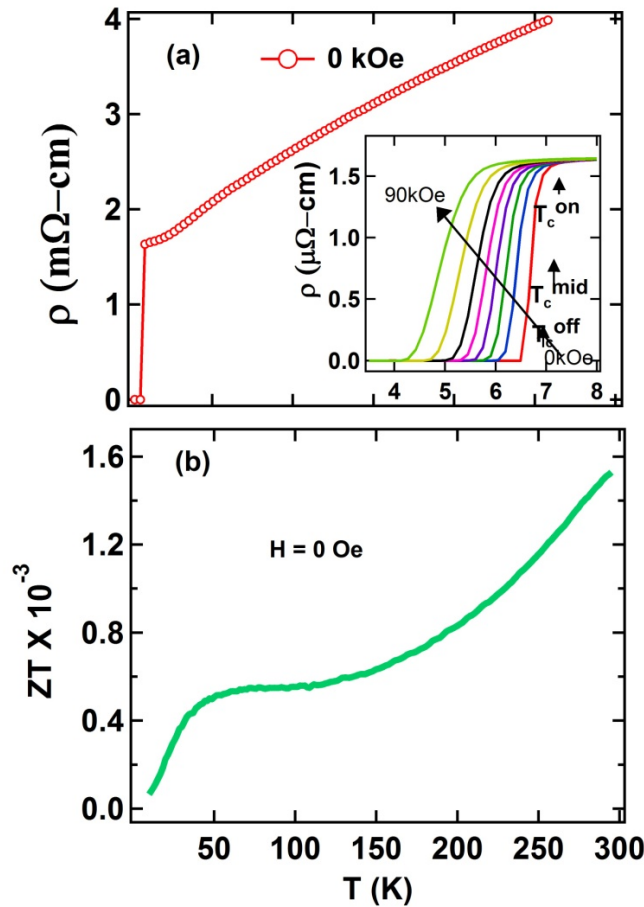


Figure 3: (a) shows ρ vs T plots at zero field in superconducting state. Inset shows resistivity plots at various magnetic fields ranges from 0-90kOe. (b) Figure of merit (Z) as a function of temperature.

Now, electron-phonon coupling strength is described by the ratio of T_c/T_F , [27] that is ~ 0.01 for this compound, this may suggest weakly correlated superconductor. Compound $KFe_{1-x}Se_y$ is also an example of weakly correlated iron superconductor, its ratio is found to be 0.04 [27]. Inset of FIGURE 2(b) shows temperature dependent of Seebeck coefficients plots in superconducting state at different applied fields, the transition temperature from normal to superconducting state shifts to lower temperature as applied magnetic fields increases, like resistivity behavior in superconducting state. The Seebeck coefficients changes abruptly from positive to zero value of S at T_c in zero field measurement. FIGURE 3(a) shows electrical transport curves at zero magnetic fields with temperature from 2K to 300K. Resistivity drop abruptly to zero at transition temperature ($T_c \sim 6.5$ K). Inset shows transport measurement under magnetic fields, the transition temperature shifts to lower temperature as field increases, similar to Seebeck coefficient measurements. Figure of merit for thermoelectric materials defines the thermal to electrical conversion efficiency, FIGURE 3(b) displays figure of merit (ZT) as function of temperature, calculated by using formula $ZT = S^2\rho/\kappa$. The moderate value of $ZT \sim 1.5 \times 10^{-3}$ is observed at room temperature.

4. CONCLUSIONS

In summary, polycrystalline sample of Nb_2PdS_5 was prepared successfully via solid state reaction method. Thermal conductivity curve show typical trend of metal. Seebeck coefficient measurements confirm positive charge carriers (holes) are present in normal state for thermal transport and at transition temperature T_c changes abruptly. In electrical-magneto transport study, metallic nature is to be observed in normal state and superconducting transition temperature suppresses with increasing magnetic fields. A lower value of figure of merit is estimated for this compound.

5. ACKNOWLEDGMENTS

AKY would like to acknowledge the UGC-startup grant (project No. F.30-303/2016 (BSR) for supporting to create lab facility. VSB would like to thank to UGC India for RGNF.

References

- [1] Zhang Q, Li G, Rhodes D, Kiswandhi A, Besara T, et al. Superconductivity With Extremely Large Upper Critical Fields in $\text{Nb}_2\text{Pd}_{0.81}\text{S}_5$. *Sci Rep.* 2013;3:1446.
- [2] Yu H, Zuo M, Zhang L, Tan S, Zhang C, Zhang Y. Superconducting Fiber With Transition Temperature up to 7.43 K in $\text{Nb}_2\text{Pd}_{X}\text{S}_5$ ($0.6 < X < 1$). *J Am Chem Soc.* 2013;135:12987-12989.
- [3] Jha R, Tiwari B, Rani P, Kishan H, Awana VPS. Robust Superconductivity With Large Upper Critical Field in Nb_2PdS_5 . *J Appl Phys.* 2014;115:213903.
- [4] Huang H, Tan M, Ji P, Duan H, Gao X, Hu X, et al. Interesting Diameter-Dependent Upper Critical Field in $\text{Nb}_2\text{Pd}_{0.77}\text{S}_5$ Superconductor. *J Supercond Nov Magn.* 2016;29:309-313.
- [5] Ning W, Yu H, Wang N, Liu Y, Han Y, Yang J, et al.. Nonlinear Transport in Quasi-One-Dimensional Nb_2PdS_5 Nanowires. *Appl Phys Lett.* 2014;105:172603.
- [6] Yadav AK, Sharma H, Thakur AD, CV, Tomy. *Mater Chem Phys.* 2015;164:46-50. doi:
- [7] Park E, Lu X, Ronning F, Thompson JD, Zhang Q, et al. Spectroscopic Evidence for Two-Gap Superconductivity in the Quasi-1D Chalcogenide $\text{Nb}_2\text{Pd}_{0.81}\text{S}_5$. *J Phys Condens Matter.* 2015;30:165401.
- [8] Jiang Y, Zhang X, Khim S, Bhoi D, Kim KH, et al. Unconventional Andreev Reflection on the Quasi-One-Dimensional Superconductor $\text{Nb}_2\text{Pd}_{X}\text{S}_5$. *AIP Adv.* 2016;6:045210.
- [9] Luetkens H, Xu X, Yang JH, Baines C, Amato A, et al.. Nodeless Superconductivity in Quasi-One-Dimensional Nb_2PdS_5 : A μ SR Study. *Phys Rev B.* 2015;91:100504.
- [10] Goyal R, Awana VPS, Patnaik S, Shruti. Unusual Non Saturating Giant Magneto-Resistance in Single Crystalline Bi_2Te_3 Topological Insulator. *Journal of Magnetism and Magnetic Materials.* *Phys C.* 2017;428:213-218.

- [11] Ning W, Yu H, Liu Y, Han Y, Wang N, et al. Aluminium Acetylacetonate Ligands Passivation for CSPBBR3 Nanocrystals With Improved Stability and Photoluminescence. 2023.
- [12] Park E, Lee S, Ronning F, Thompson JD, Zhang Q, et al. Spectroscopic Evidence for Two-Gap Superconductivity in the Quasi-1D Chalcogenide nb2pd0.81s5. *J Phys Condens Matter*. 2018;30:165401.
- [13] Goyal R, Srivastava AK, Mishra M, Gupta G, Jha R, Awana Vps. X-Ray Photoelectron Spectroscopy, Magnetotransport and Magnetisation Study of nb2pds5 Superconductor. *J Supercond Novel Magn*. 2018;31:943-949.
- [14] Shen CY, Si BQ, Bai H, Yang XJ, Tao Q, et al. PD Site Doping Effect on Superconductivity in Nb 2 PD 0.76 S 5. *EPL*. 2016;113:37006.
- [15] Zhou N, Xu X, Wang JR, Yang JH, Li YK, et al. Controllable Spin-Orbit Coupling and Its Influence on the Upper Critical Field in the Chemically Doped Quasi-One-Dimensional Nb 2 Pds 5 Superconductor. *Phys Rev B*. 2014;90:094520.
- [16] Chen Q, Shen CY, Yang XH, Yang XJ, Li YP, et al. Effect of Ruthenium Doping on Superconductivity in Nb 2 Pds 5. *J Phys Conf Ser*. 2017;807:052002.
- [17] Chen Q, Yang X, Yang X, Chen J, Shen C, et al. Enhanced Superconductivity in Hole-Doped Nb2pds5. *Front Phys*. 2017;12:127402.
- [18] Goyal R, Awana VPS. Effect of NI Doping at PD Site in nb2pds5 Superconductor. *J Supercond Nov Magn*. 2017;30:3355-3360.
- [19] Kaushik V, Venkateshwarlu D, Venkatesh R, Ganesan V. Enhancement of the Upper Critical Field (HC2) In nb2pd(s0.9te0.1)5 Superconducting Fibers. *AIP Conf Proc*. 2020;2265:030566
- [20] Neu J, Graf D, Wei K, Gaiser A, Xin Y, et al. Superstructures and Superconductivity Linked With PD Intercalation in Nb 2 PD X SE 5. *Chem Mater*. 2020;32:8361-8366.
- [21] Zhan P, Wang Z, Liu Y, Wang J, Xing Y. Integrating Quasi-One-Dimensional Superconductors on Flexible Substrates. *AIP Adv*. 2022;12:065319.
- [22] Poole CP Jr., Farach HA, Creswick RJ. *J Supercond*. 2007;22.
- [23] Putti M, Marrè D, Napoli F, Tassisto M, Manfrinetti P, et al.. Electron Transport Properties of MGB2 in the Normal State. *Eur Phys J B*. 2002;25:439-443.
- [24] Damodara Das V. An introduction to thermoelectric, Aparna publications India 1995;34:534.
- [25] Behnia K, Jaccard D, Flouquet J. On the Thermoelectricity of Correlated Electrons in the Zero-Temperature Limit *J Phys Condens Matter*. 2004;16:5187.
- [26] Kaushik V, Venkateshwarlu D, Venkatesh R, Ganesan V. Superconducting and Normal State Properties of Quasi-One-Dimensional nb2pd(s0.9te0.1)5 System. *J Solid State Chem*. 2022;305:122652.
- [27] Wang K, Lei H, Petrovic C. Quantum Transport of Two-Dimensional Dirac Fermions in Srmbi 2 *Phys Rev B*. 2011;84:220401.